CHANGES OF MAGNETIC PROPERTIES AND SURFACES CONDITION DUE TO THERMAL TREATMENT OF FeNbCuBSi RIBBONS

Beata Butvinová[1], Pavol Butvin[1], Magdaléna Kadlečíková[2], Marek Kuzminski[3], Kornel Csach[4]

[1]*Institute of Physics Slovak Academy of Sciences, Bratislava, Slovakia,*
[2]*Institute of Electronics and Photonics FEI, Slovak Univ. Technol., Bratislava, Slovakia,*
[3]*Institute of Physics Polish Academy of Sciences, Warsaw, Poland,*
[4]*Institute of Experimental Physics Slovak Academy of Sciences, Košice, Slovakia*
E-mail: beata.butvinova@savba.sk

Received 30 April 2012; accepted 03 May 2012.

1. Introduction

Rapidly quenched magnetic metallic ribbons are a focus for researchers and technicians already for a long time because of their excellent soft-magnetic properties. The major components (e.g. Fe) are chemically reactive and the large surface to volume ratio enables various surface effects to be significant. Although indications of surface-based intrinsic macroscopic stresses affecting magnetic properties of nanocrystalline ribbons (e.g. magnetic anisotropy [1]) were observed early enough, such effects still appear to be considered but marginally. Though at annealing, macroscopic stress does not tend to achieve a low-level equilibrium as as-cast microscopic stress does, but the former can increase due to ribbon's vulnerability to preserve or even build up its macroscopic heterogeneity (e.g. surface crystallization, oxidation) [2, 3]. Magnetostrictive low-Si alloys clearly show susceptibility to different ambience at thermal treatment and the hysteresis loops show up accordingly different [4] and display characteristic magnetoelastic anisotropy (slant loops) after non-vacuum annealing, whereas high Si (> 12 at.%) alloys show little effect. Our main motivation is to find out whether certain surfaces conditions could be indicative of macroscopic stress generation in a medium-Si, medium-magnetostrictive Fe-Nb-Cu-B-Si alloy.

2. Experimental Details

The Finemet family $Fe_{72.5}Nb_{4.5}Cu_1B_{12}Si_{10}$ ribbon was prepared by planar-flow casting in air. As-cast samples with a thickness around 21 μm were cut to strips of 10 cm length and 1 cm genuine width. The target magnetic properties together with the nanocrystalline state were obtained by annealing at 540°C for 1 or 2 hours in different ambience (Ar and N_2) and tensile stress annealing at 540°C for 2 hours (in Ar, under 100 MPa). No devoted surface-cleaning procedure has been applied prior to annealing or measurement. Nitric acid-based lye was used for surface removal by etching. The investigated ribbon is a positively magnetostrictive material (coefficient $\lambda_s = 8\times 10^{-6}$ after annealing). Hysteresis loops were recorded using a digitizing hysteresisgraph at ac (20 Hz) sinusoidal *H* excitation (along the ribbon long axis) in Helmholtz drive coils. Raman spectroscopy (RS) investigation of strip surfaces exploited the confocal system with 632.8 nm monochromatic laser radiation; the beam applied 15 mW power focused onto spot with ~10 μm diameter. The static domain structure was studied by means of computer-aided magneto-optic Kerr effect (MOKE) assembly [5]. Simple domain structures comprising 180° walls are easy to interpret: The largest (magnetic) image contrast is obtained if the maximum magneto-optical sensitivity (MMOS) is set by operator parallel to major domain magnetization direction – the easy magnetization direction.

3. Results and Discussion

Nanocrystalline $Fe_{72.5}Nb_{4.5}Cu_1B_{12}Si_{10}$ ribbon annealed in Ar or N_2 manifests slant hysteresis loops in contrast to the upright one (not shown but quite alike Fig. 1a) obtained after vacuum annealing. The tilt of slant loops is proportional to hard-ribbon-axis (HRA) anisotropy attaining energy density up to 100 J/m^3. The anisotropy after vacuum annealing is feeble since it is easily overwhelmed by applying modest compressive stress (e.g. by resin potting [6]) and the genuine upright loop gets slant. However, when annealed (in Ar) under longitudinal tensile stress, this material acquires strong, relatively homogeneous within the ribbon volume, "creep-induced" magnetic anisotropy directed along the ribbon axis (giving upright loop). Thus we chose stress annealing to discern better the expected influence of surfaces. The result of various anneals presents different magnetic anisotropy as shown in Fig. 1. Loops of the ribbons annealed in Ar or N_2 ambient without stress show similar tilt. Earlier studies demonstrate the tilt to come from compressive stress exerted by surfaces on the ribbon interior [6] and MS and CEMS investigation [7] revealed preferred surface crystallization as the possible source.

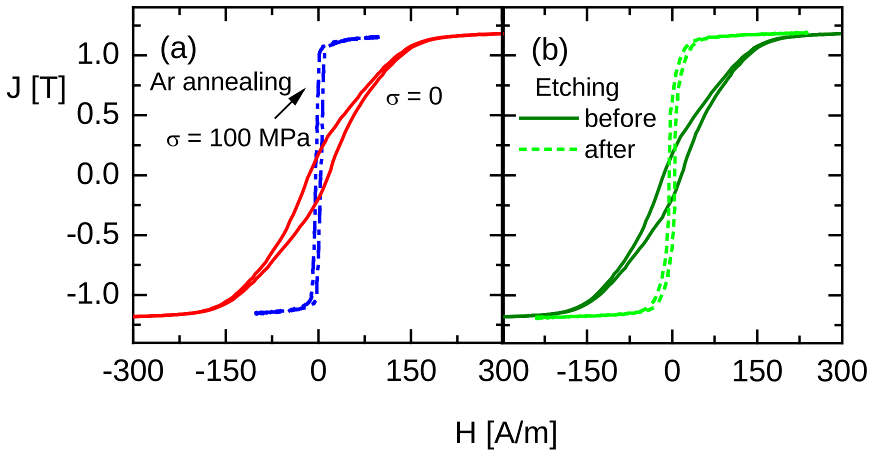

Fig.1: *Hysteresis loops (20Hz) of strips annealed at 540°C: (a)-for 2 hours in N_2,, no tension and in Ar at 100 MPa tensile stress; (b)-for 1 hour in Ar and the same after etching.*

The upright loop after stress-annealing (Fig. 1a) does not reveal what is seen on corresponding domain structure (Fig.2-left) – typical domain pattern of magnetically harder area showing no clearly preferred surface anisotropy. The surface removal makes the strong induced volume anisotropy to emerge (Fig.2- right). Unlike the surface domain structure, the loop represents an integral sample response and it shows but modest changes (therefore not shown in Fig. 1) after the 12.5% thickness removal: The loop still straightens up slightly which demonstrates removal of compressive stress originally exerted by surfaces, simultaneously showing that the ensuing magnetoelastic anisotropy was present in this sample too but as a minor only component. The other change is the reduction of coercivity by 28% (from 4.1 to 2.9 A/m). The magnetic hardness of the genuine surface can be explained by ferrous oxides detected by RS (see Fig.3) – the oxides generally display lower saturation but far larger coercivity than the basic Finemet. Still, there could be other reasons for the relative hardness that are not detected by RS. Unfortunately, RS is neither capable of confirming the removal of oxides since etched surfaces respond by huge photoluminescence, which obscures any well discernible peaks in the spectrum. Here we rely on the domain images that show "magnetically soft and clean" surface after etching in Fig. 2 right. The wheel-side surface removal resulted in an image very similar to air-side one - Fig. 2 right.

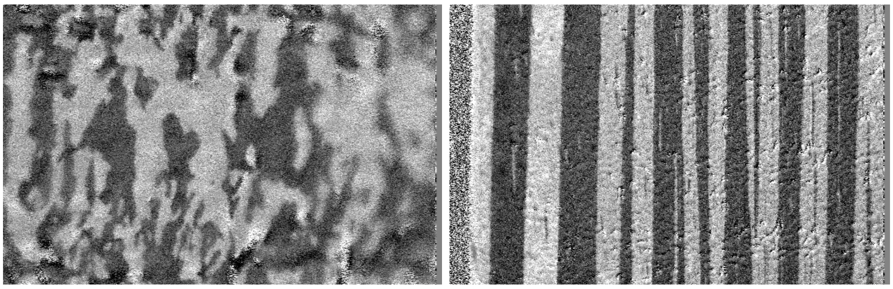

Fig.2: *Domain structure of stress-annealed $Fe_{72.5}Nb_{4.5}Cu_1B_{12}Si_{10}$ showing air side: left - magnetically-hard surface prior to etching, right – after etching showing volume domains (real horizontal dimension 2 mm-left and 6 mm- right, ribbon axis and MMOS vertical).*

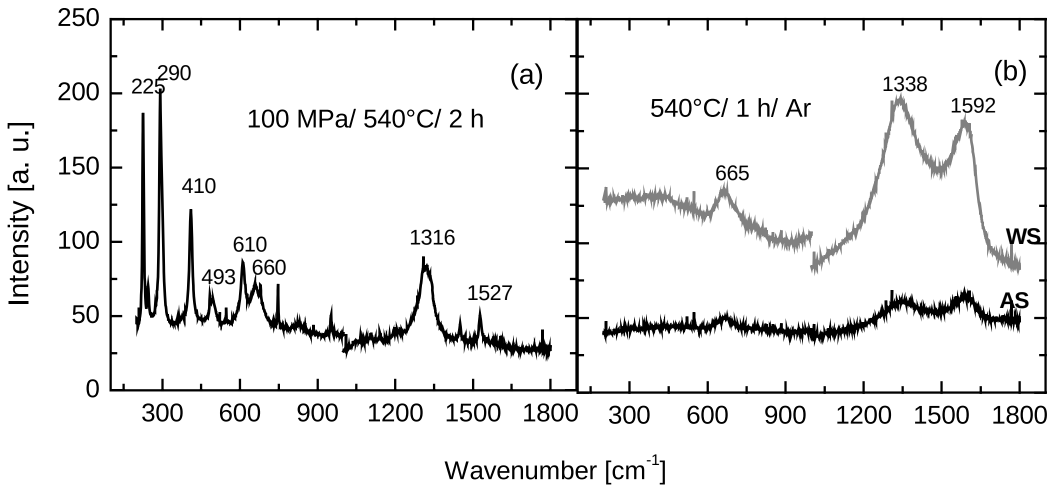

Fig.3: *Raman spectrum of the tensile stress-annealed (a) and no-stress annealed sample (b). The whole abscissa range is scanned in two separate runs, which meet at 1000 cm^{-1}*

RS of the stress-annealed strip revealed peaks attributable to α-Fe_2O_3 and γ-Fe_2O_3 [8] that appeared with various intensity on more places of both surfaces - Fig. 3a. No-stress annealing in N_2 as well as in Ar largely shows little-prominent peak at 665 cm-1 and graphitic carbon (GC) 1300-1600 cm^{-1} twin peak (see Fig. 3b) observed more generally within dark blemish spots on ribbon surface. The GC is probably of extrinsic origin – ribbon surface pollution by a random aerosol [9] or furnace resident. It nevertheless seems to enable forming of the structure responding to RS at 665 cm^{-1} on otherwise Raman-unresponsive glossy ribbon surface. The little-prominent peak can be tentatively ascribed to Fe_3O_4 oxide blend [8]. Two distinct conditions point to the different RS response to no-stress and stress annealing: Despite similar Ar atmosphere, the longitudinally stressed surfaces cannot relax the mutual stress to ribbon interior the same way as “free” surfaces can and diverse furnaces were used for the different annealing. No deeper-reaching interpretation is available so far. Domains displayed by Fig. 4 for no-stress annealed strip clearly demonstrate the magnetic difference to the stress-annealed sample (Fig. 2). The genuine air-side surface shows distinctive transversal (to ribbon axis) domains manifesting their source - the HRA anisotropy inferred above from the characteristic tilt of corresponding loop (Fig. 1b). No discernible domain structure is seen toward ribbon edges. Since rotation of magneto-optical sensitivity (to vertical) did not help to see clear domains, we conclude that some non-magnetic stain was present at the edges. Though the assumption of GC to form the stain is at hand, we did not follow this “non-magnetic” hint further for there is an alternative explanation (bad illumination of the non-planar strip). Far more important is the change caused by etching, which reduced strip thickness by 16%. The result is principal reconstruction of anisotropy – from HRA to easy-ribbon-axis anisotropy as seen when comparing left and center image of Fig.4. The corresponding loop follows suit – its tilt is almost removed (Fig. 1b). The wheel-side surface shows similar result (Fig. 4 right) although it did not enable to estimate the change since the genuine surface gave poor contrast only (not shown).

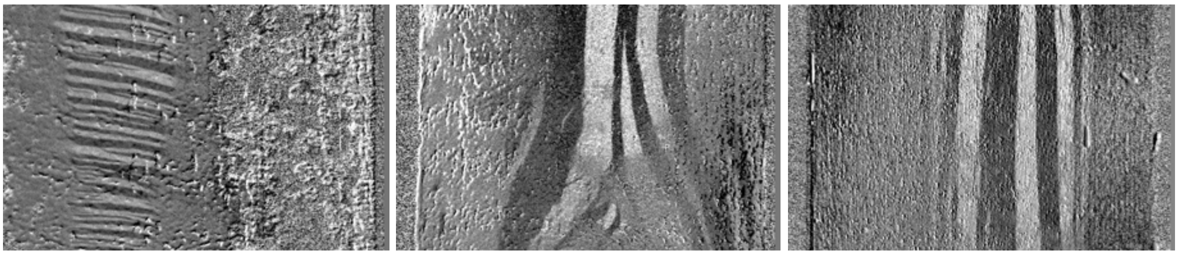

Fig.4: *Domain structure of Ar annealed (no stress)* $Fe_{72.5}Nb_{4.5}Cu_{1}B_{12}Si_{10}$ *showing: left - air side (AS), no etching; center – AS, after etching; right - wheel side (WS), after etching. (real horizontal dimension 6 mm – left and 10 mm – center and right; ribbon axis and magnetooptical sensitivity vertical besides left one where this is horizontal).*

4. Conclusions

Different annealing behavior of surfaces and ribbon interior as observed in the material studied leads to twofold sort of influence:

- Direct effects as oxidation-caused magnetic hardening, which is observed as contribution to coercivity.
- Indirect effects mediated via macroscopic mutual stress resulting in specific magnetoelastic contribution to anisotropy, which is revealed by a slant hysteresis loop.

Surface removal proved that the above effects come primarily from the ribbon surfaces. The surface effects inevitably result from non-vacuum annealing but can be rendered minor by stronger volume anisotropy as shown by intentional creep-induced anisotropy. The identified ferrous oxides and the suspect extrinsic graphitic carbon take its part in forming of the heterogeneity however, the mechanism of action is still not clear in enough detail.

Acknowledgement

The authors are grateful for partial financial support by grants No. VEGA-2/0056/11, VEGA-2/0056/12, VEGA- 1/1102/11 and VEGA- 1/1103/11.

References

[1] B. Hofmann, T. Reininger, H. Kronmüller, *phys.stat.sol.* (a) **164,** 247 (1992).
[2] R. Schäfer, A. Hubert, G. Herzer, *J. Appl. Phys.* **69,** 5325 (1991).
[3] B. Butvinová, P. Butvin, R. Schäfer, *Sens. Actuators* A **106**, 52 (2003).
[4] P. Butvin, J. Sitek, B. Butvinová, E. Illeková, *J Phys. IV France* **8**, Pr-123 (1998).
[5] M. Kuzminski, J. Fink-Finowicki, A. Siemko, *Electronic Horizon* **53**, 87 (1992).
[6] P. Butvin, B. Butvinová, Z. Frait, J. Sitek, P. Švec, *J. Magn. Magn. Mater.* **215-216**, 293 (2000).
[7] S. Havlíček, O. Schneeweiss, T. Žák, Y. Jirásková, A. Buchal, *J Phys. IV France* **8**, Pr-75 (1998).
[8] D.L.A. de Faria, F.N. Lopes, *Vibrational Spectroscopy* **45**, 117 (2007).
[9] S. Metres, B. Dippel, A. Schwarzenböck, *Aerosol Sci.* **35**, 347 (2004).